RESISTIVE WALL MODE PHYSICS AND CONTROL CHALLENGES IN JT-60SA HIGH BETA-N SCENARIOS

L. PIGATTO, T. BOLZONELLA, G. MARCHIORI
Consorzio RFX
Padova, Italy
Email: leonardo.pigatto@igi.cnr.it

N. AIBA, N. HAYASHI, M. HONDA, G. MATSUNAGA, M. TAKECHI
National Institutes for Quantum and Radiological Science and Technology (QST)
Naka, Japan

YQ. LIU
General Atomics
San Diego, United States

S. MASTROSTEFANO
DEIM, Università della Tuscia
Viterbo, Italy

F. VILLONE
Consorzio CREATE, DIETI, Università degli Studi di Napoli Federico II
Napoli, Italy

Abstract

The superconducting tokamak JT-60SA is being built in Naka (Japan) under the Broader Approach Satellite Tokamak Programme jointly by Europe and Japan, and under the Japanese national programme. JT-60SA has an important supporting mission for the development of fusion energy: designed to achieve long pulses (100 s) and break-even equivalent plasmas, challenging high β operation beyond the no-wall limit. It will help in both the exploitation of ITER and in the definition of an optimized DEMO design. The device will be equipped with off-axis Negative-NBI at 0.5 MeV beam energy, allowing current profile tailoring for Advanced Tokamak scenarios with fully non-inductive current drive. The focus of the work is set on high β_N scenarios, in which kink-like instabilities (e.g. one or more RWMs) are potentially unstable and possibly lead to disruptions. In the framework of a joint European-Japanese collaboration, coordinated effort on MHD stability and control modeling is ongoing for the safe realization and exploitation of high β_N plasmas. These scenarios offer a great opportunity to test and verify present models of RWM physics. The drift-kinetic damping model in particular will be considered in the present work, with a stability study in Scenario 5–like plasmas carried out with MARS-F/K. The challenge of active control is also addressed, taking advantage of the set of RWM Control Coils that JT-60SA will have. A dynamic simulator, based on the CarMa code, has been developed for feedback control modeling. A demonstration of this tool is given in one of the aforementioned plasmas, showing potential applications, results and latest developments.

1. INTRODUCTION

The superconducting tokamak JT-60SA is being built in Naka (Japan) as part of the Satellite Tokamak Project (STP) of the Broader Approach (BA) agreement within European Union and Japan [1][2]. It has an important supporting mission for the development of fusion energy: designed to achieve long pulses (up to 100 s) and break-even equivalent plasmas, it will help in both the exploitation of ITER and in solving key issues for the future DEMO devices. JT-60SA will be able to explore plasma configurations with shape factor up to $S=q_{95}I_p/(aB_\varphi) \sim 7$ (where B_φ is the toroidal field, I_p the plasma current in MA, a is the minor radius, q_{95} the safety factor at 95% of the toroidal flux) and aspect ratio down to $A \sim 2.5$.

Additional heating and current drive systems will provide up to 41 MW for 100s, divided between 34 MW neutral beam injection and 7 MW of ECRF. The off-axis Negative-NBI at 0.5 MeV beam energy in particular, allows current profile tailoring for Advanced Tokamak scenarios with fully non-inductive current drive. In the present work the focus is set on high β_N scenarios, in which one or more Resistive Wall Modes are potentially unstable. RWM instabilities are ideal MHD pressure driven modes that develop when the normalized kinetic to magnetic pressure exceeds the so-called no-wall limit. According to present understanding three factors are of key importance for determining these stability limits: the current profile (i.e. the plasma internal inductance), the pressure profile (i.e. the pressure peaking factor) and the minimum value of the safety factor profile (i.e. q_{min}).

RWM stabilization is one of the crucial tasks for future fusion devices, particularly when aiming at steady state operation and high plasma pressure. For this reason the problem of understanding the physical mechanisms lying underneath these modes, including the possible damping channels has been challenged in theory and experiments [3]. Dealing with Resistive Wall Modes, which although slowed down by passive structures are still strong ideal instabilities, can be a complex task and has been done in different ways, mainly using passive and active techniques. Passive stabilization is usually sought with a combination of plasma flow and different damping mechanisms such as viscosity or the so-called kinetic resonance with particle drift motions. Active control of RWMs, on the other hand, has been studied and tested in a variety of schemes from the virtual shell idea to mode control and its evolutions [4][5][6][7]. RWM feedback control will also be possible on JT-60SA thanks to the presence of a stabilizing plate and a set of active coils, as shown in FIG. 1. Dedicated modelling tools are being developed including a realistic three-dimensional description of the passive and active structures [8]. It is foreseeable that future control techniques for fusion devices will take advantage of both passive and active stabilizing effects, in order to improve plasma performance.

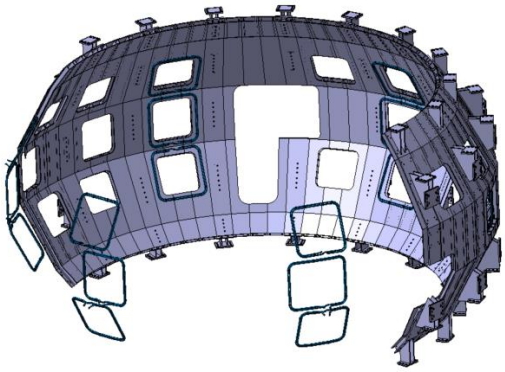

FIG. 1. 3D representation of the JT-60SA stabilizing plate and RWM control coils

The reversed magnetic shear Scenario 5 (I_p = 2.3 MA, B_t = 1.72 T) [9] belongs to those that should establish the base for high β_N, fully non-inductive current drive operation on JT-60SA. The implemented equilibrium in particular has been obtained from an integrated modelling simulation performed with the CRONOS suite of codes which used the transport model CDBM for simulating heat transport whereas the density profile has been prescribed. The goodness of this transport model and in general of CRONOS for performing JT-60SA extrapolations was verified with JET and JT-60U data [10]. The boundary parameters, and in particular the pedestal top pressure, have been obtained from the reference Scenario 5. The scenario implemented for the present work represents a version with lower input power developed using 17 MW of NBI and 7 MW of ECRH, therefore leaving sufficient power management flexibility for mode and profile control purposes, and resulting in a normalized β value of ~ 3.6.

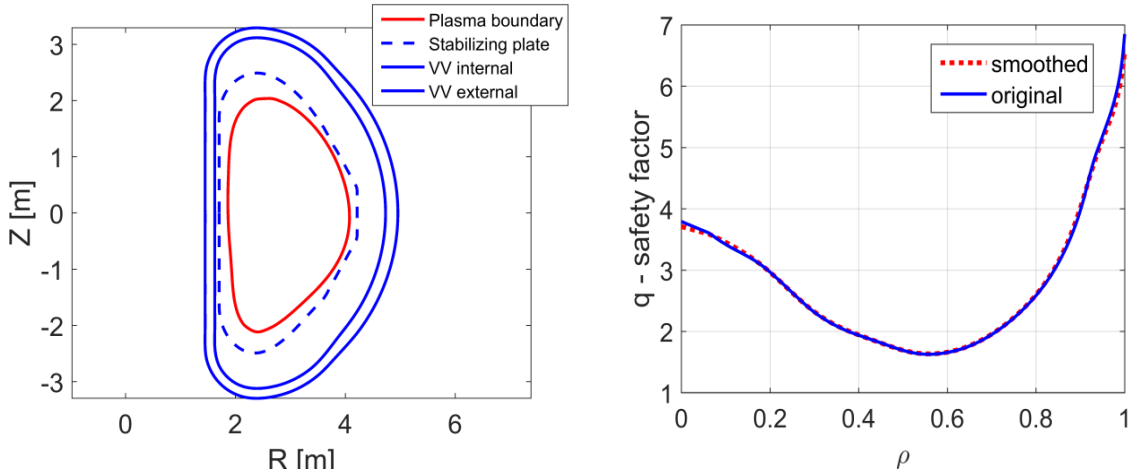

FIG. 2. Left: Plasma boundary, first wall (stabilizing plate) and vacuum vessel contours. Right: Safety factor profile before (blue) and after (red dashed) smoothing of plasma boundary and internal profiles

In particular the present work studies the global MHD stability of the Scenario 5 representative described above, starting from ideal MHD limits. The implemented plasma and wall geometry is shown in FIG. 2 (left). RWM physics is investigated with the codes MARS-F/K [11]. The first part of the work reports considerations on ideal

stability limits for the target plasma, with respect to previous calculations [12], widening the range of considered parameters. The latest results are shown on the side of RWM kinetic damping, with the progressive introduction of kinetic resonances. The challenge of active control is then addressed, taking advantage of the set of RWM Control Coils that JT-60SA will have. A dynamic simulator has been developed for feedback control modelling [13]. The core of this flight simulator is a state space representation of the system (Plant) given by the CarMa code [14], which is integrated with a complete representation of the digital control system. This allows for a realistic description of the passive and active structures with the effects of 3D geometry on plasma dynamics. In the initial version a current input model has been implemented, thus allowing a straightforward implementation of the desired control schemes with the implicit assumption that the current control loop is capable of meeting the requests. A demonstration of this tool is given in one of the aforementioned plasmas, showing potential applications. Some of the latest results obtained with the dynamic simulator include the eigenvalue study of the full closed-loop system with the implementation of the 18 active coils, representing an evolution of [15].

2. IDEAL KINK AND FLUID RWM DESCRIPTION

As a first step in understanding the stability properties of the aforementioned equilibrium the no-wall and ideal-wall pressure limits have been assessed with a series of pressure scans. The no-wall limit has been found to be $\beta_{nw} \approx 1.96$, which is consistent with results for similar equilibria. For the ideal-wall limit calculation two positions have been considered for the wall. The one closest to the plasma (r/a = 1.119) can be considered an optimistic case while the second wall position (r/a = 1.205) a more realistic situation with respect to the position of the stabilizing plate. In the present work a 2D thin wall has been implemented which does not take into account the real three-dimensional characteristics of the stabilizing plate. These 3D features can have an important impact on plasma stability and on the control capabilities of the system; this topic will be addressed in the following sections. The results of the pressure scans are reported in FIG. 3 and summarized in TABLE 1.

TABLE 1 IDEAL-WALL LIMIT

	r/a = 1.205	r/a = 1.119
β_{iw}	4.3	5.4

With a $\beta_N = 3.6$ the reference equilibrium is in between the calculated limits, in the so-called wall stabilized region, where the ideal wall stabilizes the external kink. Since any realistic wall has a finite resistivity this mode is not fully stabilized but slowed down from Alfvénic time scale to the wall penetration characteristic time. The time constant of the simplified 2D boundary has been set to $\tau_W \approx 100\ ms$, to match the order of magnitude of the wall time calculated with the 3D code CarMa [8]. All the results presented with normalization to τ_W or τ_A , can be rescaled to any calculated wall time for comparison with other codes and data.

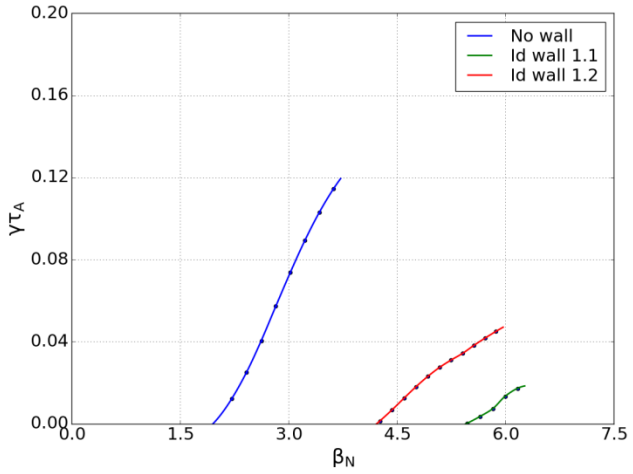

FIG. 3. No-wall and Ideal-wall stability limits calculated for n=1 with constant plasma current. Two ideal wall positions are shown: b/a=1.205 (red) and b/a=1.119 (green)

As a starting point to the discussion on rotational stabilization, and for later comparison with the drift-kinetic case, simplified plasma rotation profiles have been introduced with the fluid model. A viscous damping approximation has been used at first which, although crude, will be used to highlight the effect of different rotation profile shapes.

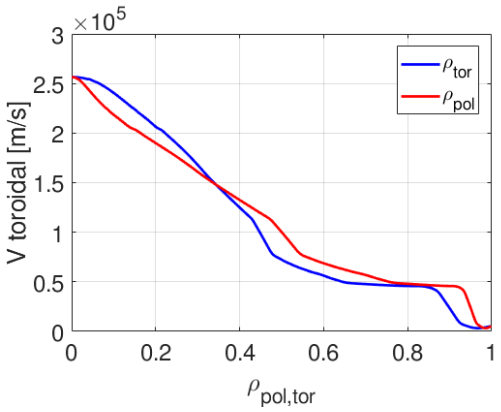

FIG. 4. Rotation profile calculated for JT-60SA beam configuration. Methodology can be found in [16].

Plasma rotation has been varied in magnitude in the interval $\Omega_0/\omega_A = 0 - 0.1$, comparing the results with constant rotation and with the profile calculated for JT-60SA reported in FIG. 4. The viscous damping term enters the momentum equation as: $\nabla\vec{\Pi} = -\rho\kappa_{\|}|k_{\|}v_{th,i}|\vec{v}_{\|}$, where the strength parameter $\kappa_{\|}$ is varied between 0.1 and 1.5. A comparison of the two cases is shown in FIG. 5, where the stronger damping expected with $\kappa_{\|} = 1.5$ is clearly highlighted. The same comparison has been carried out with constant plasma rotation, resulting in an even stronger damping even at lower rotation values. This suggests an important contribution of plasma rotation towards the outboard of the torus. For the following study of drift kinetic damping of the RWM however, the more realistic rotation profile given in FIG. 4 shall be used, keeping the smallest viscous damping coefficient ($\kappa_{\|} = 0.1$).

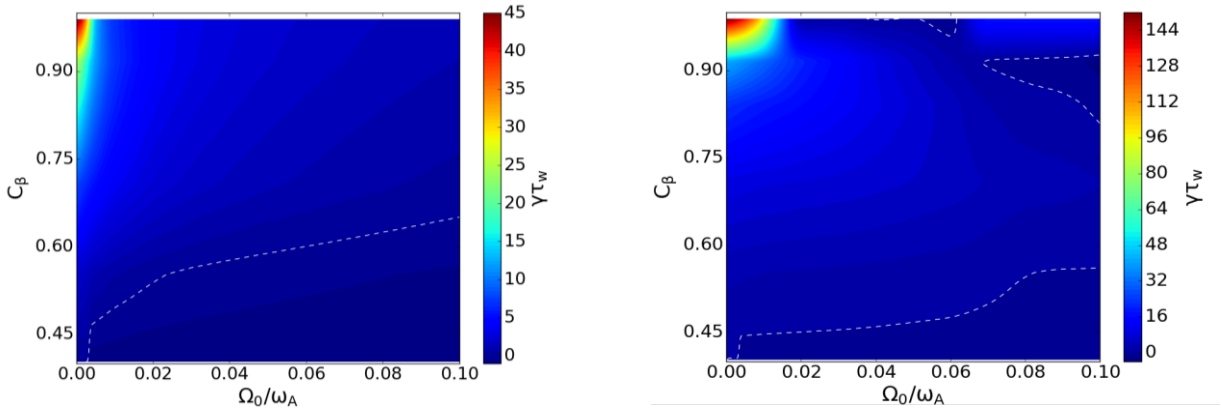

FIG. 5. Contour plots of the real part of the normalized RWM eigenvalue with varying rotation speed and plasma pressure. The fluid model is used with a small viscous damping coefficient $\kappa_{\|} = 1.5$ (left) $\kappa_{\|} = 0.1$ (right). Both plots use rotation profile in FIG. 4.

3. RWM STABILITY WITH DRIFT-KINETIC CONTRIBUTION

In the present paper the MARS-K self-consistent approach is used to introduce drift-kinetic effects [11]. Thermal ions and electrons have been introduced as a first step, assuming a Maxwellian distribution and focusing on the resonance between the mode and the precession motion of trapped particles banana orbits. For EPs a slowing-down distribution is assumed in particle energy space and isotropic distribution in particle pitch-angle [17]. In the present work the toroidal $E \times B$ flow of the plasma is varied in magnitude, following the same procedure described above and using the rotation profile reported in FIG. 4. The key role is played by the resonance between the $E \times B$ flow and the characteristic drift frequencies of thermal ions and/or EPs. The matching between $E \times B$ flow and these frequencies results in the drift kinetic resonance. The precessional drift frequency for thermal and hot ions, the bounce frequency for thermal ions and the ion diamagnetic frequency for the target plasma are shown in FIG. 6. The right panel of FIG. 6 also reports the scan of the kinetic contribution with the multiplying factor α_D, representing the evolution of the mode eigenvalue from the fluid description ($\alpha_D = 0$) to the drift kinetic one ($\alpha_D = 1$).

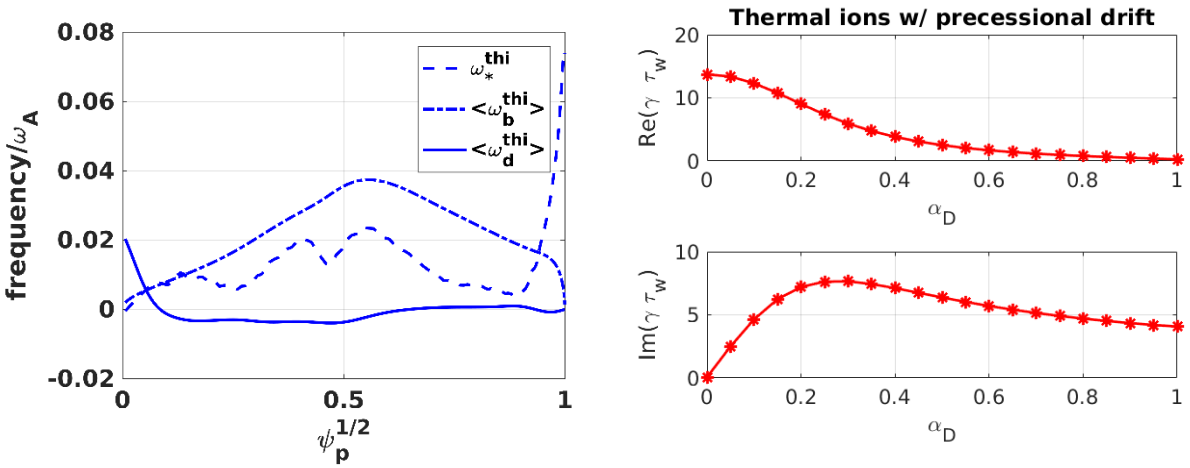

FIG. 6. Left: Frequencies for thermal ions averaged over velocity space and flux surface: precessional drift frequency (solid), bounce frequency (dot-dashed) and diamagnetic frequency (dashed). Right: scan of the drift kinetic contribution.

Interestingly enough for the target plasma the precessional drift of thermal ions has a stabilizing effect even without rotation, as can be seen from the left-side plot of FIG. 6. The blue solid curve, representing normalized precession drift frequency for thermal ions, crosses $\omega = 0$ more than once and the profile flattens to zero for $\sqrt{\psi_p} > 0.5$. This suggests a strong resonance when $\omega_{E\times B} \approx 0$ over the whole radius. This is understood from the mode-particle resonance contribution to the perturbed kinetic energy which can be written for the case shown above. RWM stability can be determined by the generalized dispersion relation described in [18] and [19], in particular resonance occurs for small values of the denominator of the following relation, simplified for the case of precession drift resonance only.

$$\delta W_k \propto \frac{n\omega_{*N} + \left({}^{\epsilon_k}/_{T} - {}^{3}/_{2}\right)n\omega_{*T} + n\omega_E - (\omega - i\gamma)}{n(\omega_d + \omega_E) - (\omega - i\gamma)}$$

Where $\omega_{*N,T}$ are the diamagnetic drift frequencies due to density and temperature gradients, ${}^{\epsilon_k}/_{T}$ the particle kinetic energy normalized by the temperature, $(\omega - i\gamma)$ is the mode growth rate and frequency, n the toroidal mode number, ω_E the $E \times B$ rotation frequency and ω_d the bounce-orbit averaged trapped-particle toroidal precession drift frequency.

4. ACTIVE STABILIZATION OF RESISTIVE WALL MODES

A simplified plasma description, given by the MARS-F code, has been coupled to a detailed representation of the RWM Control Coils and Stabilizing Plate (SP), which is modeled with all its 3D features such as thickness and ports. A 3D view of these structures has been given in FIG. 1. In the following, the error field correction coils will

not be used and have been therefore excluded from the model. The results that will be described in the present work refer to the equilibrium configuration reported above, scaled to $\beta_N \sim 2.7$. In the model the most unstable eigenvalues can be selected and identified as RWMs from their growth rates and from the comparison with the 2D problem solved by MARS-F. Synthetic magnetic probes have been added to the 3D model to document e.g. how the most unstable RWM would appear. From a total of 108 magnetic probes available in JT-60SA for real time measurements, 39 will be placed on the stabilizing plate close to the plasma on the low field side. A coil current input model has been built with the CarMa code output. This allows the straightforward implementation of the desired control schemes with the implicit assumption that the current control loop is capable of meeting the requests. A more detailed discussion concerning the current requirements will be given in the following sections. An open-loop version of the model has been used to evaluate free-mode evolution, spatial distribution and harmonic content. Interestingly enough, due to the 3D features of the stabilizing plate, which exhibits holes with no periodical symmetry, the expected unstable RWM is actually split in two modes, with different imaginary part (phase) and slightly different growth rates. These latter are found to be $\gamma_1 = 551\ s^{-1}$ and $\gamma_2 = 402\ s^{-1}$.

In JT-60SA feedback control of RWMs will be possible thanks to a set of 18 active coils located on the inner side of the stabilizing plate. A plasma response model provided by the CarMa code has been implemented for RWM active control studies. This model based approach has already been successfully adopted and validated in the experimental device RFX-mod [13]. The final aim of the JT-60SA modelling work introduced here is the development of a full simulator, including a plasma response model with a 3D description of the passive structures, sensors, signal processing blocks and controller. In principle, the model can provide a number of virtual measurements so as to obtain a detailed map of the plasma response. Moreover, a vacuum version allows a full spatial and dynamic characterization of the magnetic field produced by the actuators in the presence of non-axisymmetric passive structures. As a first step, an eigenvalue analysis of the open loop (i.e. without any active external action) plasma response has been accomplished, as described in the section on RWM stability, and two unstable eigenvalues have been found. When moving to a possible active control strategy, as a first attempt a modal control scheme has been chosen, focusing on the n=1 harmonic of the tangential component of the magnetic field. This is proposed in agreement with experimental results obtained by the same approach in different experimental devices [20] that showed how this choice guarantees to reduce the coupling between the actuators and the feedback signal. The Discrete Fourier Transform (DFT) of the signals from the upper and lower sensor arrays is calculated and the control relevant harmonics selected. A corresponding harmonic signal is obtained at the controller output, whose inverse transform is then evaluated along the toroidal coordinate, taking into account the coil periodicity (in this case equal to the sensor one). In the following closed-loop studies of the system an ideal current controller is assumed and purely proportional gains will be applied. The system is schematically represented in FIG 7.

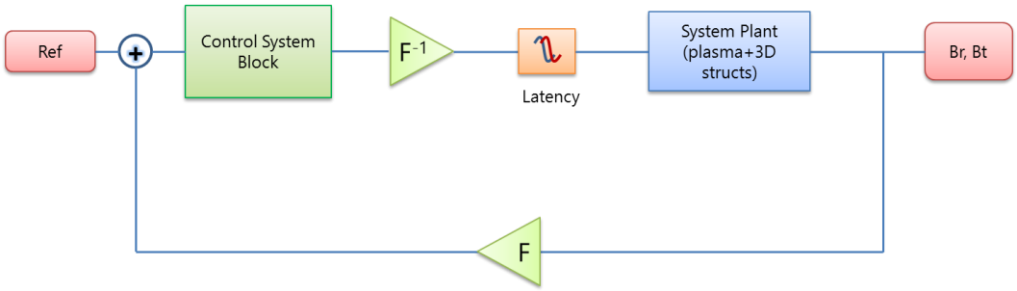

FIG 7. Block diagram of feedback system implemented in the closed loop model of RWM control

An eigenvalue study of the system has been performed to evaluate the critical gain required for mode stabilization. A constant phase shift has been applied to the action of each coil in order to maximize its effect. These phases have been calculated during the open-loop preliminary analyses with a helical reference signal. The gain scan reported in FIG. 8 shows that the unstable modes are fully stabilized with a proportional gain of $7 \times 10^6 \frac{A}{T}$. The applicability of such a gain cannot be assessed with instruments such as eigenvalue analyses and requires challenging the problem from the point of view of time simulations.

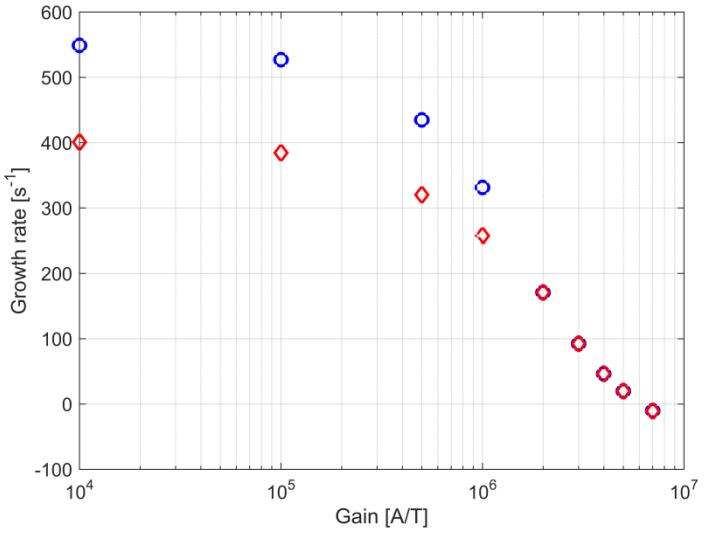

FIG. 8. Eigenvalue study of the full system with proportional controller. Two unstable n=1 modes are found and stabilized at the same time.

The closed-loop system shown in FIG 7 has been implemented as a Matlab Simulink model to obtain a dynamic simulator for RWM control studies. A gain scan similar to that shown in the eigenvalue study has been performed around the supposed critical value. The time simulations have confirmed the previously calculated stabilizing gain. As for the previous eigenvalue analyses, the tangential magnetic field is used as feedback variable for the time simulations. An initial free evolution phase, has been set to allow the desired mode to develop from the random initial condition (generated t = 0 s) up to $B_t \sim 5\ mT$. The feedback loop is then closed with three different gains: $4 \times 10^6 \frac{A}{T}$, $6 \times 10^6 \frac{A}{T}$ and $8 \times 10^6 \frac{A}{T}$. The stabilizing threshold is found in between the last two values. It is worth noting that two different dynamics are found in the closed-loop part of the simulation. The mode undergoes a fast initial phase (0.01 s – 0.012 s) during which its amplitude rapidly decreases. Once the faster components have decayed the growth rate stabilizes around the expected eigenvalue. The full output of the time simulation has been considered to investigate the current required by the applied control scheme. For the most stabilizing case ($K_p = 8 \times 10^6 \frac{A}{T}$) the simulated magnetic field (tangential component), as measured by all the sensors, and the current flowing in each active coil is shown in FIG. 9. The resulting Ampere-turns are compatible with the JT-60SA sector coil and power supply system design [21].

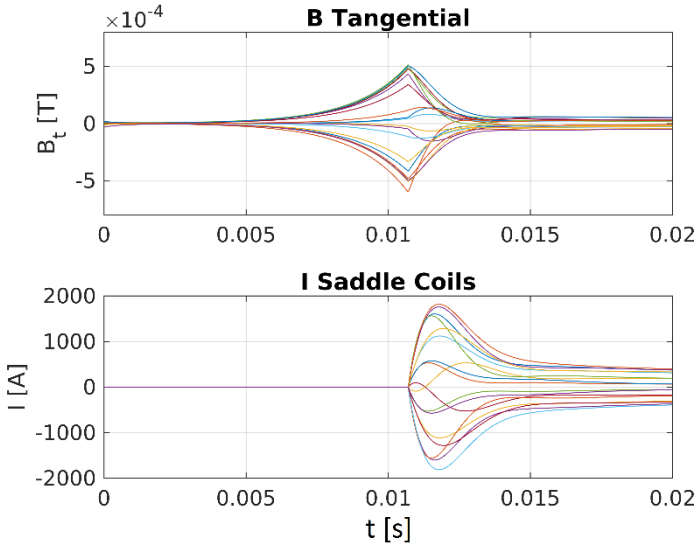

FIG. 9. Tangential field (upper plot) and coil current (lower plot) for each sensor and each active coil, example taken from the highest gain case K_p=8×10^6.

5. CONCLUSIONS

Resistive Wall Mode stability has been studied for a representative non-inductive scenario for JT-60SA. The boundaries between which RWM stabilization is foreseeable have been conservatively evaluated and promising initial results have been obtained considering the effect of drift kinetic resonances on mode stability. Stabilization of the n=1 RWM with external coils has been successfully simulated in the present work, for the first time with the implementation of the full system. The plasma coupled to the 3D structures, although rescaled to lower pressure with respect to the target, represents and upper bound situation in terms of the mode growth rate. Extensive optimization work is ongoing to upgrade the model described above in terms of plasma pressure and controller detail.

ACKNOWLEDGEMENTS

This work has been carried out within the framework of the EUROfusion Consortium and has received funding from the Euratom research and training programme 2014-2018 under grant agreement No 633053. The views and opinions expressed herein do not necessarily reflect those of the European Commission. The authors gratefully acknowledge members of the JT-60SA Integrated Project Team for data exchange and fruitful discussions.

REFERENCES

[1] H. Shirai et al., Nucl. Fusion 57 (2017) 102002
[2] G. Giruzzi et al., Nucl. Fusion 57 (2017) 085001
[3] M.S. Chu, M. Okabayashi, Plasma Phys.Control.Fusion. 52 (2010) 123001
[4] V. Pustovitov, Plasma Phys. Controlled Fusion. 44 (2002) 295
[5] P. Zanca et al., Nucl Fusion 47 (2007) 1425
[6] T. Bolzonella et al., Phys. Rev. Lett. 101 (2008) 165003
[7] T. Bolzonella et al., Fusion Eng. Des. 82 (2007) 1064-1072
[8] S. Mastrostefano et al., Fusion Eng. Des. 96 (2015) 659-663
[9] JT-60SA Research Plan: http://www.jt60sa.org/pdfs/JT-60SA_Res_Plan.pdf
[10] N. Hayashi et al., Nucl. Fusion 57 (2017) 126037
[11] Y. Liu et al., Physics of Plasmas 15 (2008) 112503
[12] L. Pigatto et al., "Resistive wall mode stability in JT-60SA high β_N scenarios", 43rd EPS Conference on Plasma Physics (Leuven, Belgium,2016)
[13] G. Marchiori et al., Nucl. Fusion 52 (2012) 023020
[14] M. Ariola et al., Control Engineering Practice 24 (2014) 15-24
[15] Bolzonella, T et al., "Securing high β_N JT-60SA operational space by MHD stability and active control modelling", Proc. 26th IAEA Fusion Energy Conf. (Kyoto, Japan, 2016)
[16] M. Honda et al., Nucl. Fusion 54 (2014) 114005
[17] Y. Liu et al., Plasma Phys. Controlled Fusion. 52 (2010) 104002
[18] M. S. Chu et al., Physics of Plasmas 2 (1995) 2236
[19] Y. Liu et al., Physics of Plasmas 15 (2008) 092505
[20] P. Zanca et al Plasma Phys.Control.Fusion 54.9 (2012) 094004
[21] Ferro A. et al., IEEE Transactions nn Plasma Science, Vol. 46, No. 5, (2018), 1670-1677